Available online at www.sciencedirect.com
ScienceDirect
Procedia Engineering 146 (2016) 75 – 82
Procedia Engineering
www.elsevier.com/locate/procedia

8th International Cold Climate HVAC 2015 Conference, CCHVAC 2015

Research on the heat transfer rules of natural convection in a building with single heat source

Naiyan Zhan, Yue Xu, Di Wang, Wubo Zhou, Hao Lv

School of Municipal And Environment Engineering Department, Jilin Jianzhu University, Jilin, China

Abstract

Taking buildings' cooling problem as the background, the natural convection were numerically simulated in a cavity with single heat source using SIMPLE algorithm with a QUICK scheme. The temperature field, flow field and rules of heat transfer were studied. The results showed that two symmetrical vortex appeared in a single heat source with the different ratio of length and height. With the increase of the ratio, vortex's number unchanged, and shape became wide. The influence of the heat source on around became weak with the increase of the aspect ratios. After considering the radiation on the building walls, the distribution of each section temperature changed. When the ratio of length and height became smaller, the distribution changed obviously. On the contrary, it had a little change. The ratio of radiation to convection basically was stable at 0.42, radiation had a greater impact to heat transfer.

Peer-review under responsibility of the organizing committee of CCHVAC 2015

Keywords: Building, Heat source; Convection; Radiation; Lateral walls

1. Introduction

Today, energy problem was one of the major challenges in the society, energy conservation and emissions reduction caused more people's attention. However, with the human living standard gradually improving, we must ensure the construction environmental comfort conditions with energy conservation and emissions reduction. Therefore, building energy efficiency and the research of building environment comfort must be closely combined. The study of natural convective thermal dissipation had important theoretical and realistic significance to improve indoor air environment, saving building energy and inhibit pests spread.

Corresponding author. Tel:15143091179, fax:+0-000-000-0000
E-mail address: velon0066@sina.com

Peer-review under responsibility of the organizing committee of CCHVAC 2015
doi:10.1016/j.proeng.2016.06.355

There were a number of related researches on this topic. As early as 1901, Benard found it that the atmospheric temperature difference would produce thermal convection. Krishnamurti, one of the earlier researchers about Rayleigh Benard convection, observed Rayleigh Benard convection-vortex forms through the experiment. Man studied heat transfer of natural convection in a square cavity with a heat source. Manab studied the influence of the tilt angle. Sharif simulated heat transfer of natural convection in a square cavity with a heat source and confirmed that the influence of the lateral walls on the national convection. Dong etc. confirmed the influence of geometry of the cavity. Q.W. Wang conducted experiments to study on natural convection in inclined square cavity with isolated plates. They confirmed the influence of the plate position, inclined angle of the cavity and the Rayleigh number on heat transfer. H.L. Jiang conducted experiments to study on natural convection in a rectangular cavity with scattered heat sources, and showed it that the plate temperature and heat transfer coefficient of scattered heat sources was only related to the self-heating power and heat transfer condition.

By analyzing the results mentioned above, it was found that there was rather little work on radiation coupling of convection. In this paper, the natural convection was numerically simulated in a cavity with single heat source using SIMPLE algorithm with a QUICK scheme. The influence of geometry and radiation on natural convection and interior rule were studied through simulation.

2. Mathematical formulation and method of solution

2. 1. The problem and mathematical formulation

The problem considered, as shown in Figure 1, refers to the 3-D (3-dimensional) natural convection and heat transfer in a cavity with single source. The temperature of heat source in the cavity is T_h. The temperature of the bottom plate and the temperature of the top plate are T_c (T_h>T_c). The height of the cavity is H. The length of the cavity is L. The width of the cavity is W. The height of the heat source is h(h=0.5H). The heat source lies in the center of the cavity. The air is considered as Boussinesq fluid. Prandtl number of the fluid is 0.701. The lateral walls are adiabatic. The aspect ratio parallel to the z-axis is L_z and the aspect ratios parallel to the x-axis are L_x, respectively.

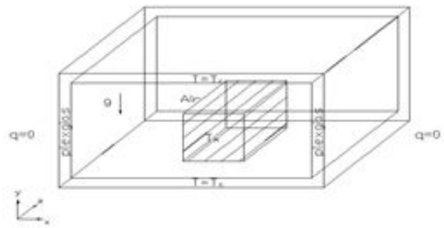

Figure 1 Geometry of the cavity

2. 2. T he governing equation

The dimensionless governing equations for the conservation of mass, momentum and energy are expressed as follows.

$$\frac{\partial U}{\partial \tau}+U\frac{\partial U}{\partial X}+V\frac{\partial U}{\partial Y}+W\frac{\partial U}{\partial Z}=-\frac{\partial P}{\partial X}+\sqrt{\frac{Pr}{Ra}}\left(\frac{\partial^2 U}{\partial X^2}+\frac{\partial^2 U}{\partial Y^2}+\frac{\partial^2 U}{\partial Z^2}\right) \qquad (1)$$

$$\frac{\partial V}{\partial \tau}+U\frac{\partial V}{\partial X}+V\frac{\partial V}{\partial Y}+W\frac{\partial V}{\partial Z}=-\frac{\partial P}{\partial Y}+\sqrt{\frac{Pr}{Ra}}\left(\frac{\partial^2 V}{\partial X^2}+\frac{\partial^2 V}{\partial Y^2}+\frac{\partial^2 V}{\partial Z^2}\right)+\Theta \quad (2)$$

$$\frac{\partial W}{\partial \tau}+U\frac{\partial W}{\partial X}+V\frac{\partial W}{\partial Y}+W\frac{\partial W}{\partial Z}=-\frac{\partial P}{\partial Z}+\sqrt{\frac{Pr}{Ra}}\left(\frac{\partial^2 W}{\partial X^2}+\frac{\partial^2 W}{\partial Y^2}+\frac{\partial^2 W}{\partial Z^2}\right) \quad (3)$$

$$\frac{\partial \Theta}{\partial \tau}+U\frac{\partial \Theta}{\partial X}+V\frac{\partial \Theta}{\partial Y}+W\frac{\partial \Theta}{\partial Z}=\frac{1}{\sqrt{RaPr}}\left(\frac{\partial^2 \Theta}{\partial X^2}+\frac{\partial^2 \Theta}{\partial Y^2}+\frac{\partial^2 \Theta}{\partial Z^2}\right) \quad (4)$$

$$\frac{\partial U}{\partial X}+\frac{\partial V}{\partial Y}+\frac{\partial W}{\partial Z}=0 \quad (5)$$

2. 3. The boundary conditions

The boundary conditions in the dimensionless form are following when the wall surface is adiabatic.

$$X=0, U=V=W=0, \frac{\partial \Theta}{\partial X}=0 \quad (6)$$

$$X=L_x, U=V=W=0, \frac{\partial \Theta}{\partial X}=0 \quad (7)$$

$$Y=0, U=V=W=0, \Theta=0 \quad (8)$$

$$Y=1, U=V=W=0, \Theta=0 \quad (9)$$

$$Z=0, U=V=W=0, \frac{\partial \Theta}{\partial Z}=0 \quad (10)$$

$$Z=L_z, U=V=W=0, \frac{\partial \Theta}{\partial Z}=0 \quad (11)$$

2. 4. The dimensionless Nusselt number

The average Nusselt number of the top wall is defined as

$$\overline{Nu}=-\frac{1}{A}\int_0^A \frac{\partial \theta}{\partial A}dA=-\frac{1}{A_{XZ}}\int_0^{L_X}\cdot\int_0^{L_Z}\frac{\partial \theta}{\partial Y}dydx \quad (12)$$

3. Mathematical formulation and method of solution

3. 1. Method of solution

The governing equations are solved in primitive variables, 3-D staggered grid based on the control volume method. The SIMPLE algorithm with a QUICK scheme is used to solve the coupled heat transfer and flow problem. For verifying the SIMPLE algorithm with a QUICK scheme, a few examples have been simulated and compared with the experimental results and simulated results conducted previously. The comparison is shown between Nusselt numbers obtained in different Rayleigh number(the grid is $100(x)\times100(y)\times100(z)$) and MARKATOS solutions given in the refs. The Nusselt numbers are listed in Table 1. The results obtained in this paper are consistent with MARKATOS solutions in refs, and the error is less than 2%. The number of grids and time step are checked in this paper. Grids are divided into equal partitions and the grids are $100(x)\times100(y)\times100(z)$. Dimensionless time is 0.01. The paper has taken the grids $200(x)\times200(y)\times200(z)$, and dimensionless time 0.001 to conduct checking. The relative difference between the Nusselt numbers in this paper and the Nusselt numbers obtained by above grids is less than 0.5%.

Ra	10^3	10^4	10^5
Nu_c(reference)	1.108	2.204	4.430
Nu_c(this article)	1.117	2.238	4.471
Error	0.81%	1.68%	0.93%

Table 1 Comparison between solutions in this paper and MARKATOS solutions in refs.

3. 2. The influence of geometry

The ratio of the height in heat source to height of the cavity is 0.5. The initial condition is zero. The four cases are conducted with the aspect ratios of L_x=1, 2, 4 and 8 with a single heat source, respectively. The temperature fields and flow fields are described in Figure 2 with single heat source.

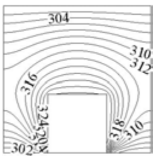

(a) *The temperature at L_x=1*

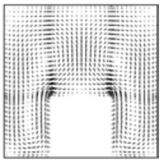

(b) The flow field at L_x=1

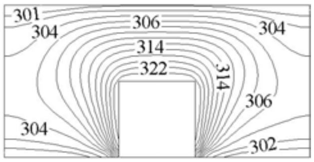

(c) The temperature at L_x=2

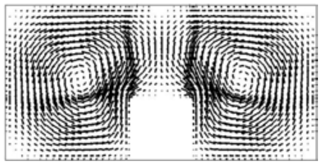

(d) The flow field at L_x=2

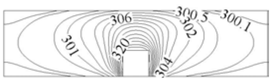

(e) The temperature at L_x= 4

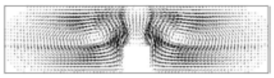

(f) The flow field at L_x=4

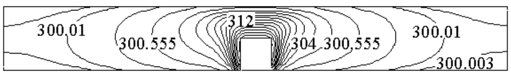

(g) The temperature at L_x=8

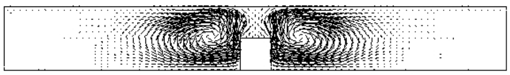

(h) The flow field at L_x=8

As shown in Figures 2, the two symmetrical vortexes appear with single heat source when the ratios are different. The number of vortexes does not vary and shape of vortexes becomes wide. With the increase of the aspect ratios the temperature of around reduces. Heat transfer becomes weak. The influence of the heat source on around becomes weak with the increase of the aspect ratios.

3. 3. The influence of radiation

The four cases are conducted with the aspect ratios of 1:1:2, 2:1:2, 4:1:2 and 8:1:2, respectively. There is single heat source. The ratio of the height of heat source to height of cavity is 0.5. The initial condition is zero. The temperature fields and flow fields at *Ra*=3000 are described in Figure 3,4,5,6.

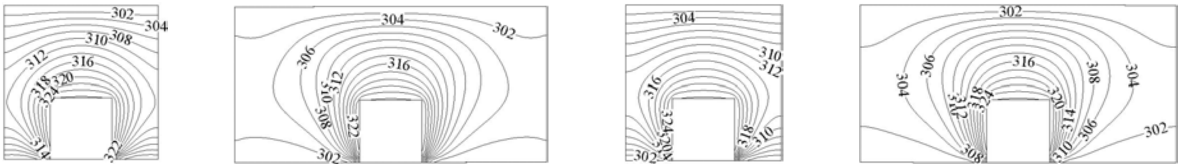

(a) (b) (c) (d)

(a) The temperature field at X=L_x/2 with radiation
(b) (c) The temperature field at X=L_x/2 without radiation

(b) The temperature field at Z=L_z/2 with radiation
(d) The temperature field at Z=L_z/2 without radiation

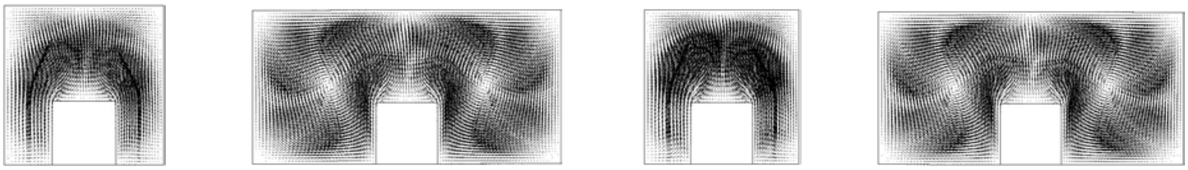

(a) (b) (c) (d)

(e) The flow field at X=L_x/2 with radiation
(g) The flow field at X=L_x/2 without radiation

(f) The flow field at Z=L_z/2 with radiation
(h) The flow field at Z=L_z/2 without radiation

Figure 3 1:1:2

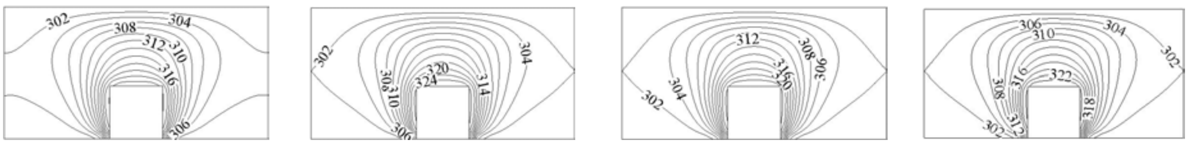

(a) (b) (c) (d)

(a) The temperature field at X=L_x/2 with radiation
(c) The temperature field at X=L_x/2 without radiation

(b) The temperature field at Z=L_z/2 with radiation
(d) The temperature field at Z=L_z/2 without radiation

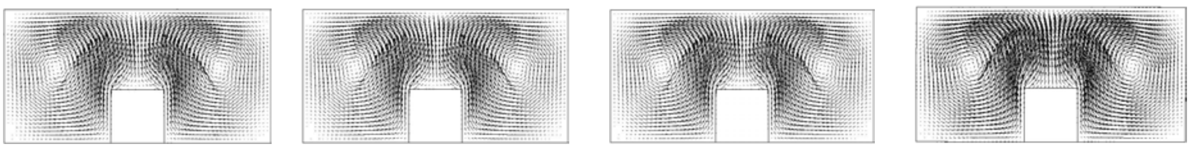

(e) (f) (g) (h)

(e) The flow field at X=L_x/2 with radiation
(g) The flow field at X=L_x/2 without radiation

(f) The flow field at Z=L_z/2 with radiation
(h) The flow field at Z=L_z/2 without radiation

Figure 4 2:1:2

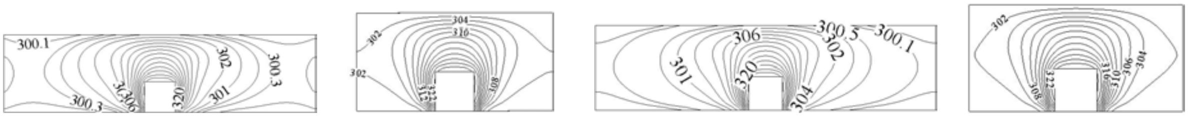

(a) (b) (c) (d)

(a) The temperature field at X=L_x/2 with radiation
(b) The temperature field at Z=L_z/2 with radiation
(c) The temperature field at X=L_x/2 without radiation
(d) The temperature field at Z=L_z/2 without radiation

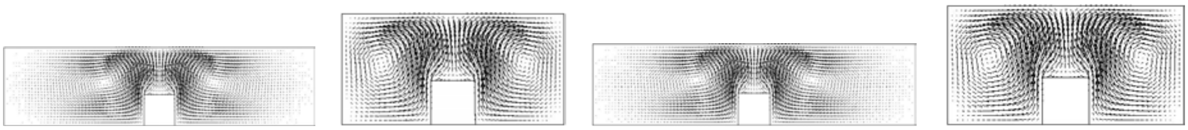

(e) (f) (g) (h)

(e) The flow field at X=L_x/2 with radiation
(f) The flow field at Z=L_z/2 with radiation
(g) The flow field at X=L_x/2 without radiation
(h) The flow field at Z=L_z/2 without radiation

Figure 5 4:1:2

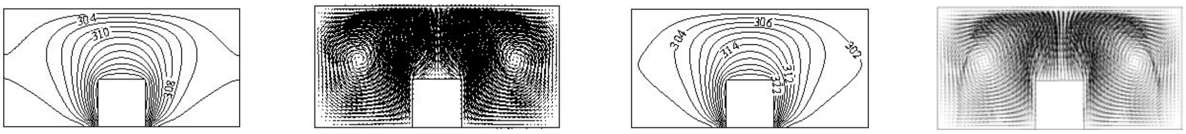

(a) (b) (g) (h)

(a)The temperature field at X=L_x/2 with radiation
(b) The flow field at X=L_x/2 with radiation
(c) The temperature field at X=L_x/2 without radiation
(d) The flow field at X=L_x/2 without radiation

(e) The temperature field at Z=L_z/2 with radiation
(f) The flow field at Z=L_z/2 with radiation

(g) The temperature field at Z=L_z/2 without radiation
(h) The flow field at Z=L_z/2 without radiation

Figure 6 8:1:2

As shown in Figures 3-6, two rolls appear parallel to the *x*-axis and *z*-axis, respectively. The rolls are close to the heat source. The rolls become wider when the the aspect ratio parallel to the *x*-axis increases. The influence of radiation on the flow field is weak.

The temperature fields of all sections vary when radiation of the cavity plates is coupled. The temperature fields are affected by radiation. The vary of the temperature fields is obvious when the ratio is small. The vary of the temperature fields is inconspicuous when the ratio is great.

The average Nusselt numbers at the top plate are described in Figure 7-9. The ratios of the average Nusselt numbers of radiation and average Nusselt numbers of convection are described in Figure 7-9. The influence of radiation on heat transfer is analyzed in this paper. The average Nusselt numbers at the top plate are expressed by blue curve with radiation. The average Nusselt numbers at the top plate are expressed by red curve without radiation. The ratios of the average Nusselt numbers of radiation and average Nusselt numbers of convection are expressed by green curve.

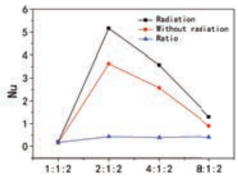

Figure 7

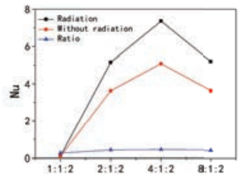

Figure 8

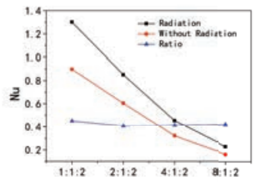

Figure 9

Figure 7 The average Nusselt numbers of the sections parallel to the x-axis
Figure 8 The average Nusselt numbers of the sections parallel to z-axis
Figure 9 The average Nusselt numbers of the top plate

The average Nusselt numbers of the sections parallel to the *x*-axis are described in Figure 7. The average Nusselt numbers of the sections parallel to the *x*-axis increase firstly, and decrease lately when radiation is not considered. The average Nusselt number of the sections parallel to the *x*-axis is 5.16 at 2:1:2. The trends of curve with radiation is similar to those without radiation. The greatest average Nusselt number of the sections parallel to the *x*-axis is 3.628 at 2:1:2. The ratios of the average Nusselt numbers of radiation and average Nusselt numbers of convection vary from 0.173 to 0.426.

The average Nusselt numbers of the sections parallel to *z*-axis are described in Figure 8. The average Nusselt numbers of the sections parallel to *z*-axis increase firstly, and decrease lately when radiation is not considered. The average Nusselt number of the sections parallel to *z*-axis is 7.357 at 4:1:2. The trends of curve with radiation is similar to those without radiation. The greatest average Nusselt number of the sections parallel to *z*-axis is 3.628 at 4:1:2. The ratios of the average Nusselt numbers of radiation and average Nusselt numbers of convection are from 0.256 to 0.446.

The average Nusselt numbers of the top plate are described in Figure 9. The average Nusselt numbers of the top plate decrease when radiation is not considered. The smallest average Nusselt number of the top plate is 0.162 at 8:1:2. The trends of curve with radiation is similar to those without radiation. The smallest average Nusselt number of the top plate is 0.23 at 8:1:2. The ratios of the average Nusselt numbers of radiation and average Nusselt numbers of convection vary from 0.406 to 0.449.

The ratios of the average Nusselt numbers of radiation and average Nusselt numbers of convection are basically 0.42 with different ratios except 1:1:2. The effect of heat transfer is affected by radiation. Radiation can not be neglected.

4. Conclusions

The natural convection has been numerically simulated in a building with single sources using SIMPLE algorithm with a QUICK scheme. The temperature field, flow field and rules of heat transfer are studied. The results show that the two symmetrical vortexes appear with a single heat source when the ratios are different. The number of vortexes does not vary and shape of vortexes becomes wide. With the increase of the aspect ratios the temperature of around reduces. Heat transfer becomes weak. The influence of the heat source on around becomes weak with the increase of the aspect ratios.After considering the radiation on the cavity wall, the distribution of each section temperature has changed. When the ratio of length and height becomes smaller, the distribution changes obviously. On the contrary, it has little change. The ratio of radiation and convection is basically stable at 0.42, radiation has a greater impact on heat transfer.

Acknowledgements

National Natural Science Foundation of China (Grant No.51206061)
Ji Lin Sheng Jiao Yu Ting Science and Technology Research [2015] (Grant No. 263)
Housing and construction department of Jilin province project.

References

[1]Dong S F. and Li Y T, Conjugate of natural convection and conduction in a complicated enclosure[J]. Int J Heat Mass Transfer, 47: 2233-2239, 2004.
[2].Fu-yun Zhao, Indoor air convection simulation and inversion polymorphism [D], Changsha: Hunan University, 2008.
[3]H.L. Jiang. and Y.G. Zhou, Study on natural convection in a rectangular cavity with heat sources. Xi'an Jiaotong University Xuebao, 32(11): 40-43, 1998.
[4]Krishnamurti R, On the transition to turbulent convection, Part 1: the transition from two to three dimensional flow. *J Fluid Mech*, 42(2): 295-307, 1970.
[5]Man Y H. and Mi J J, A numerical study on three-dimensional conjugate heat transfer of natural convection and conduction in a differentially heated cubic enclosure with a heat-generating cubic conducting body[J], Int J Heat Mass Transfer, 43: 4229-424, 2000.
[6]Manab K D. and Saran K S K, Conjugate natural convection heat transfer in an inclined square cavity containing a conducting block [J]. Int J Heat Mass Transfer, 49: 4987-5000, 2006.
[7]MARKATOS K A PERICLEOUS, Laminar and Turbulent Natural Convection in an Enclosed Cavity, Int J Heat Mass Tranafer, 27(5):755-772, 1984.
[8]Q.W. Wang, et al, Experimental Study on natural convection in a inclined square cavity [J], Journal of Engineering Thermophysics, 19(20): 204-208, 1998.
[9]Sharif M A R, Laminar mixed convection in shallow inclined driven cavity with hot moving lid on top and cooled from bottom[J]. Apply Therm Eng, 27: 1036-1042, 2007.
[10]Yang K T, Transitions and bifurcations in laminar buoyant flows in confined enclosures. ASME J Heat Transfer, 110(4): 1191-1204, 1988.